Beyond winglets: evolution of flight-related morphology in stick insects (Phasmatodea)

Yu Zeng[1,2†], Sehoon Park[1], Camille Gonzales[1],
Stephanie Yom[1], Faszly Rahim[3,4], and Robert Dudley[1,5]

[1]Department of Integrative Biology, University of California, Berkeley, CA 94720, USA
[2]Schmid College of Science and Technology, Chapman University, Orange, CA 92866, USA
[3]Centre for Insect Systematics (CIS), Universiti Kebangsaan Malaysia,
43600 Bangi, Selangor, Malaysia
[4]Islamic Science Institute (ISI), Universiti Sains Islam Malaysia,
71800 Bandar Baru Nilai, Negeri Sembilan, Malaysia
[5]Smithsonian Tropical Research Institute, Balboa, Republic of Panama
†Corresponding author: dreavoniz@berkeley.edu

Abstract

The first winged insects evolved from a wingless ancestor, but details of the transition from wingless to winged morphology remains unclear. Studying extant pterygotes undergoing secondary flight loss may help to understand such a transition in reverse temporal sequence. Stick insects (Order Phasmatodea) are characterized with slender body shape and exhibit various intermediates between transitions between fully-winged and wingless forms. Here, we studied the flight-related parameters of wings and body-leg system in different phasmids over a wing loading range from 1.4 – 2300 Nm^{-2} to address how these traits may correlate with flight evolution. Phasmid wings exhibited low aspect ratios (1.2 to 2.7) that was correlated with wing size. With reduced size, wing venation exhibited structural reconfiguration and the wingbase shifted nearer to the center of body mass, which position was highly conserved despite a wide range of variation in body shape. In addition, the masses of the wings and flight musculature are best predicted by relative wing size, and the area of the body-leg system was predominately predicted by specific allometric scaling. Our results demonstrate complex reconfiguration of the flight apparatus and body-leg system during wing loss in phasmids, albeit with some conserved features that influence flight performance.

Keywords

allometry, flightlessness, legs, sexual dimorphism, venation, wings

1. Introduction

Deriving from a single phylogenetic origin, pterygotes and their wings continue to exhibit rich dynamics on evolutionary timescales. The ancestors of winged insects were small terrestrial hexapods possessing only protowings (see Kukalová-Peck, 1983; Ellington, 1991; Dudley, 2000). And although the initial process of flight gain remains unclear, the earliest winged insects must have undergone substantial increase in wing size under selection. Once equipped with substantial wings, numerous pterygote lineages have then secondarily undergone partial or complete wing loss; ~5% of the extant pterygote fauna is flightless (Roff, 1994). The main reason underlying secondary flight reduction is likely the energetic cost for developing and maintaining the flight apparatus (e.g., wings and associated musculature), along with high energy expenditure during flight. Partial reduction or complete loss of wings has been associated with various ecological conditions, including developmental tradeoffs, enhanced female fecundity, and reduced demand for aerial mobility in montane habitats (Roff, 1994; Mani, 2013).

Partial wings presumably possess reduced aerodynamic capabilities (e.g., force generation) but may still serve locomotor functions within specific behavioral contexts, which has only been reported in derived taxa (e.g., water surface skimming in stoneflies; Marden, 2003). More often, size-reduced wings serve secondarily derived non-aerodynamic functions, such as use in protection, stridulation, and startle displays (see Dudley, 2000). Notably, one understudied behavioral context is controlled aerial descent (including parachuting, gliding, and aerial maneuvering). Empirical analyses suggest that flapping flight by pterygotes may have evolved from gliding in apterygotes via a series of intermediate morphologies with partial wings (Dudley et al., 2007; Dudley and Yanoviak, 2011). Within such a context, partial wings on a stably falling insect will interact with an upward flow field, and thus would be subject to high aerodynamic loading (Zeng et al., 2017).

A systematic examination of the transition in flight-related morphology between winged and wingless forms may help to understand the biomechanical origins of insect flight. Such an investigation may be approached at two levels. First, it is important to address features of the flight apparatus, including the wings and flight muscle, with respect to variation in relative wing size. For example, the shape and flexibility of wings are biomechanically coupled with the aerodynamics of flapping wings and body movements during flight. For fully winged insects, wing shape is often sexually dimorphic and may vary with species-specific ecology (e.g., Le Roy et al., 2019; Perrard et al., 2014); greater variation may be expected if the insects undergo drastic loss of flight capability. Also, because partial wings may interact with air flow differently than do full-sized flapping wings, the pterothoracic morphology and flight musculature may be reconfigured to power specific wing motions. Second, it is important to address the morphology of the body-leg system. The body-leg system is conventionally treated as the 'airframe' with legs omitted, but the legs are fully extended in many flying insects and thus should be incorporated aerodynamically. The body-leg system influences flight via both aerodynamic and inertial forces, which are determined by the size, shape, and mass of individual segments and their joint configurations (see Dudley, 2000). For species with partial wings, the body-leg system may serve as the dominant aerodynamic surface, assisting force production or stability via postural control and movements (Thomas and Taylor, 2001; see also below).

The stick insects (Order Phasmatodea) are known for their slender body and legs, and represent one of the few pterygote clades that have been analyzed for wing size variation within a context relevant to flight biomechanics. These insects are herbivorous and generally inhabit terrestrial vegetation, including tall tree canopies. Extant phasmids exhibit vestigial forewings and variably-sized hindwings (denoted the 'wings' hereafter), ranging from fully-sized to almost absent or vestigial wings. The processes of wing reduction and flight transition in phasmids remain largely understudied, despite the hypothesis that relaxed selection for flight (i.e., aerodynamic utility) underpins short-winged or wingless species within an arboreal context (Zeng et al., 2020).

Previous work revealed robust near-isometric scaling laws of body mass and wing area in stick insects, which allows for a relatively confident prediction of wing loading (p_w ; the ratio of body weight to the total wing area) using body length (L) and the relative wing size (Q; i.e., the ratio of absolute wing length L_w to L). The empirical prediction for wing loading is a surface defined by L and Q (the 'wing loading landscape'), which enables analysis of trait variation with respect to different stages of flight loss (**Fig. 1A**; Zeng et al., 2020). Within a more general context of insect flight, phasmids exhibit a continuous variation of wing loading, the lower range of which overlaps with that of other winged insects commonly studied for flight biomechanics (**Fig. 1B**). Previous work also revealed two 'adaptive peaks' among winged stick insects: one was associated with long-winged species, and the other with species with miniaturized wings. These two peaks were separated by an 'adaptive valley' of short-winged species with $Q \approx 0.3$ and $p_w \approx 10$ Nm^{-2}, as supported by relatively less frequent evolutionary transitions to brachypterous forms from either wingless or long-winged forms (Forni et al., 2022). A reduction of flight capability is likely associated with the morphological space characterized by $p_w < \sim 10$ Nm^{-2}. In our preliminary observations, short-winged species with high p_w performed gliding in an aerodynamic configuration different from that of long-winged species (**Fig. 2**).

On the wing loading landscape, the most general pattern is an inverse correlation between Q and L (**Fig. 1C,D**), suggesting that selection favored lower wing loading (i.e., smaller bodies with relatively larger wings) in males; a relaxation of such selection corresponds to body size increase and wing reduction in females. Nevertheless, the evolution of flight-related morphology is also subject to a variety of other selective pressures (e.g., body size; see Zeng et al., 2020).

In order to identify the principal variations of flight-related parameters with respect to evolution of wing size and wing loading, here we sampled from male and female phasmids across a wide range of wing sizes to evaluate the following features: (1) Wing shape and venational structure, which are important morphological features relative to flight biomechanics; (2) Masses of the wings and flight musculature, which influence energetic expenditure and flight performance; (3) Body plan, its mass distribution, and projected planform area of the body-leg system, which are essential for addressing the inertial and aerodynamic roles of the body-leg sections during flight (see Ellington, 1984; Dudley, 2000). Among sampled insects, the smallest p_w was ~1.4 Nm^{-2} in *Brevinecroscia* sp. males, whereas the largest was ~2300 Nm^{-2} in *Extatosoma tiaratum* females.

We analyzed the scaling of these parameters with respect to p_w, L, Q, and the absolute wing length L_w (= LQ). Based on predictions from the controlled descent of wingless insects (Zeng et al., 2017) and from a preliminary observation that reduced wings can function effectively during descent (**Fig. 2**), we predicted changes in wing morphology (i.e., in both shape and venation) given the altered aerodynamics in reduced flight. Specifically, we aimed to develop empirical models for describing the evolution of these flight-related parameters, which can then inform biomechanical analyses of phasmid flight. When possible, we compared data from phasmids with those of eight insect species from five different orders that are commonly studied for flight biomechanics.

Given sexual dimorphism in wing and body sizes, male and female insects of the same species should be treated as different evolutionary morphs. In total, our study covered 25 female and 26 male samples from 35 species. Our sampling also included the tropical stick insect *Asceles tanarata* Brock, 1999 (Brock, 1999; Seow-Choen, 2000). Native to the Malay Peninsula, *A. tanarata* consists of three subspecies distributed along an altitudinal gradient from ~50 m to ~1600 m, with wing reduction ranging from fully developed to miniaturized wings, along with substantial body size reduction (**Fig. 1E**). *A. tanarata* represents one of the few well-documented cases of discrete intraspecific variation in flight-related morphology across an environmental gradient. This species also exhibits a unique coupled reduction in wing and body size, which represents an outlier for stick insects considering the more general inverse correlation between wing and body size (**Fig. 1C,D**).

2. Materials and methods

2.1 Insect collection and husbandry

For convenience, we designate any given sex of a given species to be a 'sample' of a specific flight morph. Our sampling included a total of 51 samples (25 female and 26 male samples, including three subspecies of *A. tanarata*; 0.2 < Q < 0.85) from field-collected or captive-reared phasmids with slender bodies (but excluding the leaf insects, Family Phylliidae). Each sample was represented by data collected from all sampled specimens. For samples with more than one specimen, the mean value was used. Our analyses were built upon six main datasets covering: (1), wing shape; (2), wing venation; (3), wing and flight muscle mass; (4), size and shape of the body-leg system; (5), longitudinal mass distribution of the body-leg system; and (6), wingbase and median joint positions (see **SI Data S1**).

2.2 Morphometrics

To analyze wing morphology, we took images of fully unfolded hind wings using a digital camera (Olympus E-3; $N = 34$ female samples; $N = 36$ male samples). Insects were anesthetized either with a 5-min cold treatment (0–4 °C) or a 5-min CO_2 treatment. Two-dimensional images of wings were then extracted using Photoshop (Adobe Inc., USA), and were measured using ImageJ (Abràmoff et al., 2004) for lengths (L_w) and areas (A_w) (**SI Fig. S1D**). Wing shape descriptions followed previous methods (Ellington, 1984). Relative wing size was calculated as $Q = \frac{L_w}{L}$, where L_w is wing length and L is body length. Wing loading was calculated as $p_w = \frac{mg}{2A_w}$, where m is insect mass, g is gravitational acceleration and A_w is the wing area of one wing (see also Zeng et al., 2020).

Identification of primary radial veins followed Ragge (1955), where the anterior anal (AA) and posterior anal (PA) veins were identified using associations with axillary sclerites at wingbase (**SI Fig. S1B,C**). The variation of the number of AA veins (N_{AA}) with respect to p_w was fitted with inverse sigmoid curves using a Four Parameter Logistic Regression (R package 'dr4pl'; Ritz et al., 2015) as:

$$n_{AA} = \frac{a - d}{1 + \left(\frac{p_w}{c}\right)^b} + d \tag{1}$$

where a, b, c, and d are the four fitting coefficients.

Body sections and legs were treated as a system of cylinders, including the anterior body section (BS1) and posterior body section (BS2) as connected at the median joint (i.e., the 1st abdominal tergum; Bragg, 1997), and the six legs (see **SI Fig. S1D**). To obtain projected planforms of body and leg segments, anesthetized insects were laid dorsoventrally on a flat surface with their legs fully extended for digital imaging. Two-dimensional images of all body parts were then extracted using Photoshop (Adobe Inc., USA), and were measured using ImageJ (Abràmoff et al., 2004) for lengths and planform areas.

2.3 Mass of flight muscle

Flight muscle mass was measured in a total of 16 different samples (6 females and 4 males from six species reared in the laboratory, and 3 females and 3 males for each subspecies of *A. tanarata* collected in the field), covering a relative wing size range from 0 – 0.78, with 2 – 6 individuals per flight morph (see **SI Data S1**). We first cut off the metathorax from euthanized insects and removed muscles associated with hindlegs and the median joint. We then indirectly measured the mass of flight muscles following NaOH digestion of soft tissue, with duration of chemical treatment adjusted according to the size of wings (Q > 0.5, 12 hr; 0.3 < Q < 0.5, 2 hr; Q <0.3, 30 min) (Marden, 1987).

2.4 Mass distribution of body-leg system

The masses of two body sections and the legs were measured from deep-frozen specimens in 20 flight morphs (10 female and 10 male samples) from 12 species (**SI Data S1**). Each body part was cut from frozen specimens and measured with a portable electronic balance (PP-2060D, Acculab; accuracy of 0.001 g and linearity of ±0.004 g) in the field or with an electronic balance (R200D, Sartorius AG, Germany) in the lab. The center of mass (COM) of the body (i.e., of the head, thorax, and abdomen) was estimated from images of frozen specimens (with legs removed) balanced on a vertically oriented razor blade (**SI Fig. S1E**). Wing mass was measured from freshly euthanized specimens. Forewings were highly reduced in size (i.e., < 5% A_w and < 0.1% mass in all sampled taxa) and were thus omitted.

The total leg mass ranged from 9% – 24% of body mass (see **SI Data S1**) and was included in corresponding body sections. Based on observations of leg posture in flight (**Fig. 2**), the mass of fore- and mid-legs was included in the anterior section, and the mass of the hind-legs was included in the posterior section. The longitudinal position of the COM relative to the anterior end was calculated as:

$$P_{COM} = \frac{0.5L_1 + (L_1 + 0.5L_2)r_m}{1 + r_m} \tag{2}$$

where L is the length of a body section, subscripts 1 and 2 denote the anterior and posterior sections, respectively, and $r_m (= m_2/m_1)$ is the mass ratio of the posterior to the anterior section. The moment of inertia (MOI) of the abdomen about the insect's COM was calculated as $I = m_2 r^2$, where r is the distance from m_2 to the COM.

2.5 Statistical analyses

For phylogenetically justified correlations, we used a molecular phylogeny that includes all three subspecies of the *A. tanarata* from a previous study (**SI Fig. S1A**; Zeng et al., 2020). The phylogenetic signals for wing and body size were significant. For the species lacking molecular data, we added them as polytomous tips to the node representing the latest common ancestor on the tree. We then generated 100 random trees with randomly resolved polytomous tips. Each new node was added using the function 'multi2di' (package 'ape'; Paradis et al. 2004), and was given a branch length that was randomly drawn from a normal distribution of branch lengths with a mean of 0.1 × mean branch lengths of the original tree, and a standard deviation of 0.01 × the standard deviation of branch lengths from the original tree. We then conducted phylogenetic generalized least square (PGLS) analyses (package 'caper'; Orme et al., 2013) and ordinary generalized least square analyses (GLS). For each correlation, we ran PGLS on all random trees and summarized the results (MLλ and coefficients), which were then compared with those from GLS tests conducted without reference to the phylogeny (i.e., $\lambda = 0$).

For correlations of a given trait with respect to wing loading, we conducted sensitivity analyses using a series of generalized linear regressions to identify the potential p_w value corresponding to a critical transition in the trait. With custom-written scripts in R, we first generated a series of p_w ranges with different upper limits (denoted $p_{w(max)}$). We then examined the significance of correlations (i.e., standard errors and *P*-values of slope coefficients) with respect to p_w.

3. Results

3.1 Wing shape evolves with wing size

Among all examined phasmids, wing aspect ratio (AR) varied between 1.2 and 2.7 (male, 1.6 – 2.6; female, 1.2 – 2.7), which range was lower than in other insect taxa commonly used in flight research (**Fig. 3A**). Wings of high AR (> 2) were generally found in insects with wing loading < 10 Nm^{-2}, whereas low AR (< 1.5) was associated with female wings in the p_w range of 5 – 10 Nm^{-2} (**Fig. 3B**).

The variational pattern of AR was specific to each sex and was not correlated with body size in either sex (**SI Data S2**). On one hand, female wing AR exhibited a reduction with increasing p_w, as shown by a progressively rounder wing shape (**Fig. 3B**). Based on sensitivity analysis, this reduction corresponds to the lower limit of p_w ~2.2 Nm^{-2}, and to an upper limit of ~23 Nm^{-2}. On the other hand, male wing AR varied between 1.6 – 2.3 and was positively correlated with absolute wing length L_w (**Fig. 3C**). These evolutionary patterns in wing shape suggest significant selection for wing aerodynamic function, potentially coupled with a sex-specific body plan and flight biomechanics (see **Discussion**).

3.2 Evolution of wing venation

The first general pattern we noticed was that the number of primary radial veins was coupled with wing size, as demonstrated with exemplar wings (**Fig. 4A**). Note that female insects had more radial veins than the males with same wing loading, corresponding to a relatively greater mass allometry exponent (see Zeng et al., 2020). With PGLS analyses, we found the total number of radial veins (N_V) was more significantly correlated with wing loading and with relative wing size Q than with absolute wing size L_w (**Fig. 4B**; **SI Data S2**). With a structural design resembling a 'Chinese fan', wing length mainly equaled the length of elytrized costal veins and was also close to the length of the longest (and most costal) radial veins (AA1); it thus was not coupled with the number of radial veins, duplication of which mainly determine wing shape and chord size. As expected, the scaling exponent of N_V with L_w was only ~0.3.

The second general pattern was that the number of anterior anal (AA) veins was relatively conserved, whereas that of the posterior anal (PA) veins decreased more sharply with reduced wing size. Correspondingly, the AA veins supported the membrane region adjacent to the elytrized costal edge, whereas the PA veins supported the more posterior anal region. The number of PA veins (N_{PA}) varied between 2 – 14, exhibiting a linear correlation with p_w (**Fig. 4C**). The number of AA veins (N_{AA}) only varied between 5 – 7, which were well fitted with inverse sigmoid curves using Four Parameter Logistic Regression models and which showed sharp reductions at $p_w \approx 10$ Nm^{-2}. (**Fig. 4D**). Treating the midpoint $N_{AA} = 6$ as a critical transition, the regression models predicted the corresponding critical p_w values to be $10^{0.75}$ Nm^{-2} (i.e., 5.8 Nm^{-2}; confidence interval of 4.4 – 8.1 Nm^{-2}) for males and $10^{1.3}$ Nm^{-2} (i.e., 18.4 Nm^{-2}; confidence interval ~0 due to small sample size of $N_{AA} = 6$) in females (**SI Data S1**). With a prediction for the function of two vein groups, and especially for structural support in the downstroke by AA veins, this pattern of vein reorganization and reduction is likely coupled with changes in wing aerodynamics at low to medium-high values of wing loading (see **Discussion**).

Furthermore, as inter-vein angles are relatively conserved (e.g., 6.8˚ – 8.8˚ between radial veins in *A. tanarata*; see **SI Fig. S3D**), the gap size (or transverse distance) between adjacent veins should increase toward the wing margin, with greater distances in longer wings. Probably so as to strengthen the membrane between primary radial veins, wings of stick insect possess intercalary veins at the wing margin (**Fig. 5A**), a trait found in other orthopteroid insects. Here, we found two levels of intercalary veins (namely primary and secondary) in long wings with L_w > 20 mm, and only one level in short wings with L_w < 20 mm (**Fig. 5B**).

Overall, these trends indicate (i), a reorganization of primary radial veins (AA and PA) along the gradients of Q and p_w, and (ii) a loss of intercalary veins with decreasing L_w, which is coupled with

conservation of inter-vein angle. Lastly, we highlight that, in forms with high wing loading, wings may exhibit significant functional modification or loss of vein components, whereas those with relatively complete venation may preserve aerodynamic capacity (**Fig. 5B**).

3.3. Masses of wings and flight musculature

Wing mass reflects developmental input and is fundamental to flapping biomechanics. Our results showed that stick insect wings were heavier than wings of other sampled insects (**Fig. 6A**). Among all sampled phasmids, the mass of a single wing (m_w) varied between 0.4 mg and 0.16 g. Whereas wings longer than 5 cm generally weighed more than 0.1 g in both sexes, the wings of males exhibited a steeper reduction in mass with reducing wing size. Overall, the scaling exponents for m_w averaged 2.2 and 1.2 in male and female insects, respectively, suggesting that wing thickness potentially increases with wing length.

At the whole-insect level, stick insect wings are relatively shorter and heavier when compared with those of other winged insects (**Fig. 6B**). The relative mass of wings (m_w') reached a maximum of 6% body mass in long-winged males (Q = 0.8), and dropped to < 1% body mass in short wings with Q < 0.4. The relative mass of flight muscle was correlated with wing size and ranged between ~0% and 14% (**Fig. 6C**), values mostly below the minimum for takeoff described in other volant insects (12% – 16%; see Marden, 1987).

With phylogenetic correlations, we confirmed that the relative masses of wings and of flight musculature were both positively correlated with relative wing size (Q), but not with body size (L) or wing loading (p_w) (**SI Data S2**). These results suggest that development of wings and flight muscles are coupled in wing size evolution, and that Q is a strong predictor for wing mass and potentially wing flapping capability (see **Discussion**).

3.4 Evolution of the body-leg system

Among sampled phasmids, body aspect ratio (i.e., the ratio of length to mean diameter) varied from 10 – 56, and was positively correlated with body length in males, but not in females (**Fig. 7A**). This high range of slenderness was much larger than in other winged insects used in comparison (mostly <10 except for a dragonfly), and is perhaps among the largest in insects. Unlike the range between 15 – 56 in males, females exhibited a lower range between 10 – 25, which can be well explained by selection for fecundity.

The mass distribution of body-leg system is fundamental to understanding body posture in flight biomechanics (e.g., abdominal oscillation; **Fig. 2**). Despite variation and intersexual disparity in body shape, the longitudinal mass distribution was fairly conserved in the two sexes, albeit with females having heavier abdomens. Using a two-section model for the body, the relative mass of the anterior body section (BS1) averaged 36.7% and 39.7% in females and males, respectively. The relative mass of posterior body section (BS2) averaged 48.2% and 33.5% in females and males, respectively. The relative mass of neither section was correlated with L, Q or p_w (see **SI Data S2**). Correspondingly, the longitudinal position of the center of mass (COM) was also conserved, lying at about 50% along the body length from the anterior end of head (hereafter abbreviated as 0.50 L; range 0.47 – 0.54 L) in females, and 0.44 L (range 0.41 – 0.46 L) in males, in both cases being generally located within 0.08 L near the median joint (**Fig. 7B**). The longitudinal positions of BS1, BS2 and COM were not correlated with L, Q, or p_w (see **SI Data S2**), except for a significant reduction in males of the mass of BS2 with increasing p_w. Wing mass was < 1% of body mass in all insects and had a negligible influence on the position of COM.

Total leg mass was generally conserved and not correlated with L, Q, or p_w. However, an increase in the relative mass of legs was correlated with body miniaturization in *A. tanarata*, suggesting a specific case of developmental tradeoffs (see **SI Section A**).

The longitudinal positions of the wingbase and median joint are fundamental to stability of flight (Ellington, 1984; Dudley, 2000). Unlike the conserved mass distribution, both the wing base and the median joint shifted as wing size reduces. In long-winged phasmids, the wingbase was located at ~0.24 L from the anterior end of head, which falls in the range of 0.12 – 0.26 L reported for other volant insects (Ellington, 1984). With increased wing loading, however, the wingbase shifted posteriorly to ~0.40 L in both sexes. The same trend was found in the position of median joint, which shifted posteriorly, from ~0.40 L to ~0.48 L in males, and from ~0.40 L to ~0.50 L in females (**Fig. 7B**). As both joints link to the metathoracic segment, these shifts resulted in a relative elongation of the mesothoracic segment and longitudinal compression of the abdominal region (**Fig. 7C**). Consequentially, distance between the wingbase and COM ($d_{wb\text{-}COM}$) was reduced to ~0.15 L in both sexes (**Fig. 7D**). Similarly, the distance from the median joint to COM was reduced to ~0.10 L in both sexes. The moment of inertia (MOI) of abdomen exhibited no significant variation with respect to wing loading, despite the reduction of the BS2 mass in males (**Fig. 7E**).

Lastly, we examined the scaling of the projected planform area of body and legs, which are mainly drag-producing surfaces in flying insects but may serve as the main aerodynamic surfaces when gliding with partial wings (**Fig. 2**). We found that projected planform areas of the body and legs followed geometrical scaling and were mainly correlated with L by power-law exponents of 1.5 – 1.7 (**Fig. 8A,B**). When compared with other winged insects, the phasmids possess much greater projected body-leg area during flight than those with similar wing loading (**Fig. 8C**). For example, the total projected body-leg area in phasmids of $p_w \sim 3\ Nm^{-2}$ is at least 10 times greater than for the ladybug and crane fly of similar wing loading.

4. Discussion

These results demonstrate systematic reorganization of the flight apparatus and body plan during evolutionary loss of flight in phasmids. Numerous morphological parameters are evolutionarily correlated with wing size and wing loading (**Fig. 9**). Despite phasmid-specific morphological features (e.g., wing venational patterns and body shape) and a high variability of flight morphs on the wing loading landscape, winged phasmids evolved with a fairly conserved body plan similar to other insects. Studying phasmid flight evolution may thus be informative for addressing principles underlying insect flight evolution.

4.1 Structural reconfiguration in partial wings

Considering variation in phasmid wing shape with respect to wing loading (**Fig. 3**), the aspect ratio (AR) range of 1.2 – 2.6 was somewhat low compared to that in other flying insects (1.5 – 5.8; Bhat et al., 2019) but probably exceeds other clades in variability. In male stick insects, the positively correlation between AR and wing length L_w is likely an adaptation for enhanced aerodynamic efficiency (Kruyt et al., 2015), in accordance with the interpretation that male stick insects are under selection for dispersal capability (Zeng et al., 2020). In female stick insects, the reduction of wing AR with from low to medium-high p_w may indicate selection for non-flapping aerodynamic functions. Considering that these wings are used in various gliding behaviors (pers. obs., YZ), a low AR wing may help in drag production at high angles of attack (Ennos, 1989; Torres and Muller, 2004; Sunata et al., 2002). Why was this reduction only found in female insects? Females have a more posterior COM, and low AR wings may result in a more posterior center of aerodynamic pressure, reducing the static margin for stability (see below). Also, females are heavier than males and may have a greater demand for vertical force generation when parachuting or gliding. With little known about aerodynamics of such partial wings with low AR and operating at high p_w, kinematic data (e.g., flow fields, wing flapping kinematics, and wing deformation) along with force analysis would be necessary to further address functional significance of these differences.

In contrast to the wings of close relatives such as orthopteran and mantodean insects (Smart, 1953; Herbert et al., 2000), phasmid wings feature a narrow, elytrized costal edge that covers their slender abdomen, and the radially organized veins support the majority of wing membrane, allowing it to fold in fanlike fashion. The variation in the radial veins follows two trends: (1) stepwise reduction of functional modules along with the gradient in Q and p_w, and (2) loss of hierarchical levels with reducing wing size L_w (**Fig. 5**).

At the whole-wing level, reduction of the number of veins with decreasing Q is likely a case of truncated development. For the AA veins, which are directly associated with wing depressor muscles (**SI Fig. S1C**), reduction at medium-high p_w is likely coupled with a reduction in downstroke capability. The PP veins appear as a modularized component, which contributes to a large part of the variation in vein number and wing area (**Fig. 4A**). This variability in number may be regulated as developmental duplication, and could contribute to relatively rapid evolution of wing gain or reduction in phasmids (Zeng et al., 2020; Bank and Bradler, 2022). Although not analyzed here, miniaturized wings of $Q < 0.3$ seem to possess high variability in design and functionality (**Fig. 5B**). Over this high-p_w regime, maintenance of the complete wing membrane (such as in At3f and At3m; **SI Fig. S3A**) suggests reduced yet non-trivial aerodynamic utility.

Lastly, both wing shape and venation of partial wings may contribute to wing deformation (e.g., camber formation) during aerial descent (pers. obs., YZ). For the next step, analysis of wing flapping kinematics is necessary to address the function of different vein groups, and to biomechanically understand phasmid wing evolution.

4.2 Scaling of wing inertia and flight muscle

The positive correlation of wing mass with wing size shows that wings are not isometrically condensed as their size is reduced, or that less cuticle is put into their construction. With mean scaling exponents of 1.2 – 2.2 (**Fig. 6A**), wing mass scaling lies in between simple models assuming uniform thickness (exponent of 1) and isometric scaling (exponent of 3), suggesting that thickness increases along with wing size. Convergence of mass in long wings from both sexes (**Fig. 6B**) is in accordance with the high AR of long wings in both sexes. For shorter wings, those of female insects had greater mass, which may be associated with wider elytrized costal edges (**SI Fig. S3**). At the whole-insect level, relative masses of wings and flight musculature can be reliably predicted using Q.

Linear reduction in the relative mass of flight muscle suggests a close coupling with wing size. Reduction in flight muscle mass may be associated with loss and reconfiguration of different muscle groups, as well as with an overall reduction in wing flapping capability. Together, these data suggest a reduction of wing inertia and flapping capability as wing size decreases, which predicts less effective force production during flapping.

4.3 Changes in the body-leg system during flight loss

For the body-leg system, only the longitudinal positions of pterothoracic segments and associated joints exhibited significant variation with respect to p_w and Q. The p_w-invariant parameters (including COM position, masses of BS1 and legs, and projected planform area of body and legs) were conserved and followed specific allometries. This result suggests limited influence of selection on flight-related functions; however, aerodynamic and inertial roles of legs and abdomen can be directly regulated via movements and postural control in flight. The role of body-leg postural control in flight performed with variously sized wings could be addressed in future research.

The posterior shift of pterothoracic segments may contribute to maintenance of stability during flight performed with partial wings and reduced weight support (**Fig. 2**). Passively stable aerodynamic configurations are achieved through the moment balance between forces produced on wings and on the body-leg system (Zeng et al. 2017). Critical for such a configuration is a statically stable posture of the insect (including wings and body-leg sections) with the center of pressure located vertically above the COM (if vertically parachuting), or posterior to the COM (if gliding with a forward component of velocity). In both cases, partial wings would generate vertical forces with reduced or no flapping. Also, the demand for abdominal oscillation is likely reduced or lost altogether as flight diminishes, because wing motions are either not oscillatory or are doing so only in small amplitude.

The posteriorward shift of the pterothorax and a corresponding reduction in wingbase-COM distance (**Fig. 7**) can effectively reduce the magnitude of wing-induced moments, compensating for instability induced by wing forces. It may also shift the aerodynamic center more posteriorly and reduce the static margin (which is negative when the center of pressure is posterior to the COM), yielding better passive stability. In the direction of flight gain, a positive static margin may be necessary for flapping flight in fully-winged insects. So far, kinematics of wing flapping and flight performance have only been documented in males of a leaf insect (Boisseau et al., 2022). These predictions should be confirmed using actual body-leg postures and body kinematics, along with stability analysis, from flight of phasmids with various sized wings.

4.4 Conclusion

Compared to other commonly studied winged insects, the phasmids are characterized by relatively rounder, shorter, and heavier wings which are possibly associated with a specific wing-folding

mechanism and an overall slender body. Also, phasmids have a relatively higher projected body-leg area than other flying insects, and are thus subject to greater aerodynamic drag during flight.

Despite these lineage-specific features, phasmid wing shape and wing venation are evolutionarily correlated with wing size and wing loading. Compared with long wings, short wings are generally rounder and exhibit reorganized venation. These changes are potentially coupled with the evolutionary loss of flight, during which wing mass and flapping abilities are reduced. Phasmid bodies exhibit various level of slenderness, but the longitudinal mass distribution is relatively conserved. Nevertheless, a posterior shift in the wingbase and the median joint in short-winged species potentially indicates specific biomechanical adaptation that should be clarified by studying the aerodynamic specifics of phasmid flight.

Acknowledgments: We thank Francis Seow-Choen for helping with field work and commenting on stick insect natural history. We also thank David Wake, Paul Brock, Kipling Will, Rosie Gillespie and George Roderick for comments, and thank Datuk Monica Chia, Faye Pon, Joan Chen, Xiaolin Chen, Ho-Yeon Han, Ian Abercrombie, Yamai Shi-Fu Huang, Lin Cao, Azuan Aziz, and Juhaida Harun for help with data collection. We further thank the Sabah Parks and the Forestry Department of Pahang, Malaysia, for permission to collect insects. This research was supported by National Science Foundation (DDIG-1110855), the Museum of Vertebrate Zoology and the Department of Integrative Biology at UC-Berkeley, the Undergraduate Research Apprentice Program (URAP) of UC-Berkeley, the Society for Integrative and Comparative Biology (SICB), and the Ministry of Higher Education Malaysia [FRGS/1/2012/SG03/UKM/03/1(STWN)].

Author Contributions: Y.Z. devised experiments and performed the majority of data collection and analyses. S.P., C.G. and S.Y. contributed to data collection and morphological analyses, and F.H. contributed to field data collection. Y.Z. and R.D. contributed to writing of the manuscript.

Conflicts of Interests: The authors declare no conflicts of interests.

Data Availability: The authors confirm that the data supporting the findings of this study are available within the article and its supplementary materials.

References

Abràmoff, M. D., Magalhães, P. J. and Ram, S. (2004). Image processing with ImageJ. *Biophotonics International* **11**, 36-43.

Bank, S. and Bradler, S. (2022). A second view on the evolution of flight in stick and leaf insects (Phasmatodea). *BMC Ecology and Evolution* **22**, 1-17.

Bhat, S. S., Zhao, J., Sheridan, J., Hourigan, K. and Thompson, M. C. (2019). Aspect ratio studies on insect wings. *Physics of Fluids* **31**, 121301.

Boisseau, R. P., Büscher, T. H., Klawitter, L. J., Gorb, S. N., Emlen, D. J. and Tobalske, B. W. (2022). Multi-modal locomotor costs favor smaller males in a sexually dimorphic leaf-mimicking insect. *BMC Ecology and Evolution* **22**, 1-18.

Bragg, P. E. (1997). A glossary of terms used to describe phasmids. *Phasmid Studies* **6**, 24-33.

Brock, P. D. (1999). *Stick and leaf insects of Peninsular Malaysia and Singapore*, Malaysian Nature Society.

Dudley, R. (2000). *The biomechanics of insect flight: form, function, evolution*, Princeton University Press

Dudley, R., Byrnes, G., Yanoviak, S. P., Borrell, B., Brown, R. M. and McGuire, J. A. (2007). Gliding and the Functional Origins of Flight: Biomechanical Novelty or Necessity? *Annual Review of Ecology, Evolution, and Systematics* **38**, 179-201.

Dudley, R. and Yanoviak, S. P. (2011). Animal aloft: the origins of aerial behavior and flight. *Integrative and Comparative Biology* **51**, 926-936.

Ellington, C. P. (1984). The aerodynamics of hovering insect flight. II. Morphological parameters. *Philosophical Transactions of the Royal Society of London. Series B, Biological Sciences* **305**, 17-40.

Ellington, C. P. (1991). Aerodynamics and the origin of insect flight. *Adv. Insect Physiology* **23**, 171-210.

Ennos, A. R. (1989). The effect of size on the optimal shapes of gliding insects and seeds. *Journal of Zoology* **219**, 61-69.

Forni, G., Martelossi, J., Valero, P., Hennemann, F. H., Conle, O., Luchetti, A. and Mantovani, B. (2022). Macroevolutionary Analyses Provide New Evidences of Phasmid Wings Evolution as a Reversible Process. *Systematic Biology*.

Herbert, R. C., Young, P. G., Smith, C. W., Wootton, R. J. and Evans, K. E. (2000). The hind wing of the desert locust (*Schistocerca gregaria* Forskal). III. A finite element analysis of a deployable structure. *Journal of Experimental Biology* **203**, 2945-2955.

Kruyt, J. W., Van Heijst, G. F., Altshuler, D. L. and Lentink, D. (2015). Power reduction and the radial limit of stall delay in revolving wings of different aspect ratio. *Journal of the Royal Society Interface* **12**, 20150051.

Kukalová-Peck, J. (1983). Origin of the insect wing and wing articulation from the arthropodan leg. *Can J Zool* **61**, 1618-1669.

Le Roy, C., Debat, V. and Llaurens, V. (2019). Adaptive evolution of butterfly wing shape: from morphology to behaviour. *Biological Reviews* **94**, 1261-1281.

Mani, M. S. (2013). *Ecology and biogeography of high altitude insects*, Springer Science & Business Media.

Marden, J. H. (1987). Maximum lift production during takeoff in flying animals. *Journal of Experimental Biology* **130**, 235-258.

Marden, J. H. (2003). The surface-skimming hypothesis for the evolution of insect flight. *Acta zoologica cracoviensia* **46**, 73-84.

Orme, D., Freckleton, R., Thomas, G. and Petzoldt, T. (2013). The caper package: comparative analysis of phylogenetics and evolution in R. *R package version* **5**, 1-36.

Paradis, E., Claude, J. and Strimmer, K. (2004). APE: analyses of phylogenetics and evolution in R language. *Bioinformatics* **20**, 289-290.

Perrard, A., Baylac, M., Carpenter, J. M. and Villemant, C. (2014). Evolution of wing shape in hornets: why is the wing venation efficient for species identification? *Journal of Evolutionary Biology* **27**, 2665-2675.

Ragge, D. R. (1955). The wing-venation of the order Phasmida. *Transactions of the Royal entomological Society of London* **106**, 375-392.

Ritz, C., Baty, F., Streibig, J. C. and Gerhard, D. (2015). Dose-Response Analysis Using R. *PLoS One* **10**.

Roff, D. A. (1994). The evolution of flightlessness: is history important? *Evolutionary Ecology* **8**, 639-657.

Seow-Choen, F. (2000). *An illustrated guide to the stick and leaf insects of Peninsular Malaysia and Singapore*, Natural History Publications (Borneo).

Smart, J. (1953). The wing-venation of the migratory locust (*Locusta migratoria* Linn.) (Insecta: Acridiidae). *Proceedings of the Zoological Society of London* **123**, 207-217.

Sunada, S., Yasuda, T., Yasuda, K. and Kawachi, K. (2002). Comparison of wing characteristics at an ultralow Reynolds number. *Journal of aircraft* **39**, 331-338.

Thomas, A. L. and Taylor, G. K. (2001). Animal flight dynamics I. Stability in gliding flight. *Journal of Theoretical Biology* **212**, 399-424.

Torres, G. E. and Mueller, T. J. (2004). Low-aspect-ratio wing aerodynamics at low Reynolds number. *AIAA Journal* **42**, 865-873.

Zeng, Y., Lam, K., Chen, Y., Gong, M., Xu, Z. and Dudley, R. (2017). Biomechanics of aerial righting in wingless nymphal stick insects. *Interface Focus* **7**, 20160075.

Zeng, Y., O'Malley, C., Singhal, S., Rahim, F., Park, S., Chen, X. and Dudley, R. (2020). A tale of winglets: evolution of flight morphology in stick insects. *Frontiers in Ecology and Evolution* **8**, 121.

Main Figures

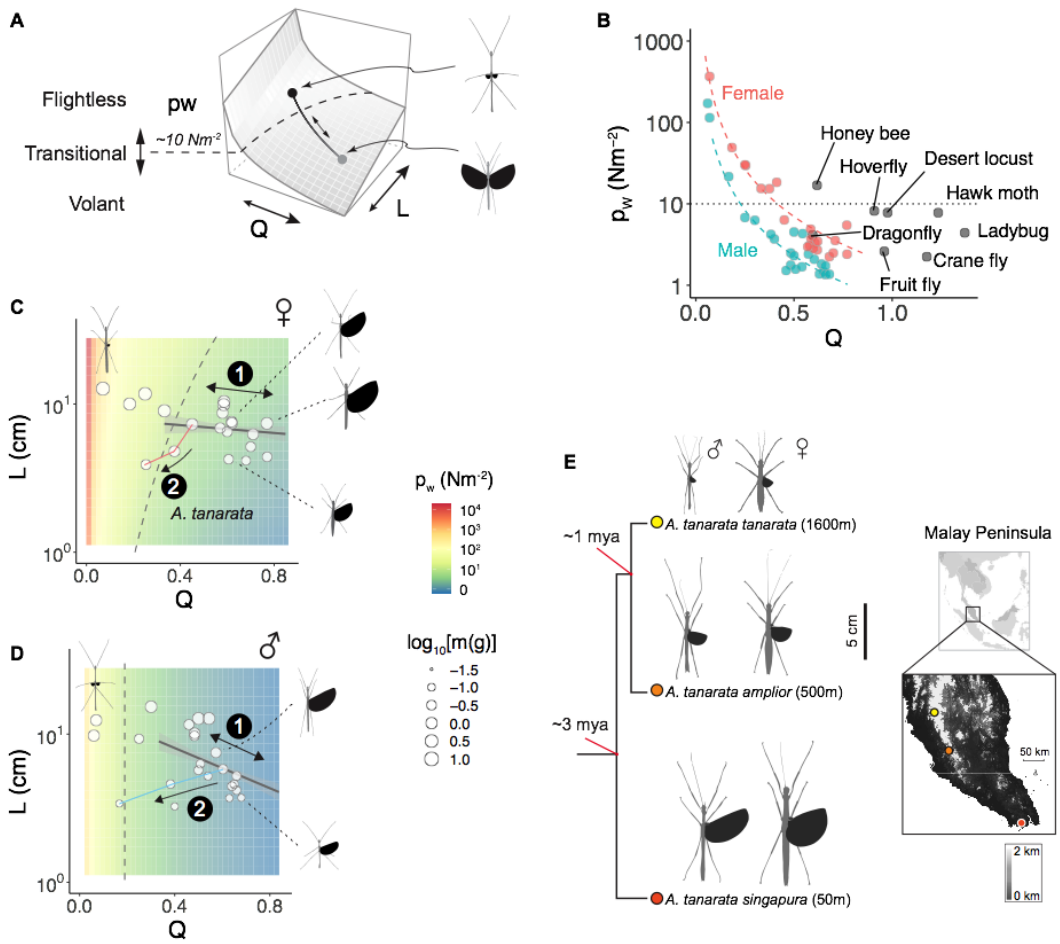

Figure 1. General patterns of flight-related morphology in stick insects.

(A) Evolution of flight morphology in stick insects can be represented by trajectories on a landscape of wing loading (p_w) defined by relative wing size (Q) and body size (L). **(B)** With decreasing wing size, stick insects exhibit a continuous increase in wing loading (data from Zeng et al., 2020), here compared with other winged insects commonly studied for flight biomechanics (see details in **SI Data S4**). **(C)** Female and **(D)** male stick insects sampled here and plotted on sex-specific p_w landscapes, with dashed contour lines showing critical $p_w \sim 10$ Nm^{-2}, with dot size representing whole-insect mass. Solid trend lines represent the general pattern – an inverse correlation between L and Q in flight evolution (based on ~270 morphologies for each sex; see Zeng et al., 2020). As an outlier, the *Asceles tanarata* subspecies (annotated with arrows) exhibited intraspecific reductions in both L and Q with increasing altitude. **(E)** Dorsally projected profiles of the three subspecies of *A. tanarata*, showing reductions in body and wing size at greater altitude. At left are the phylogenetic relationships among three subspecies, with nodes annotated with divergence time (see Zeng et al., 2020); on the right is an altitudinal map of the Malay Peninsula, annotated with locations where three subspecies were collected.

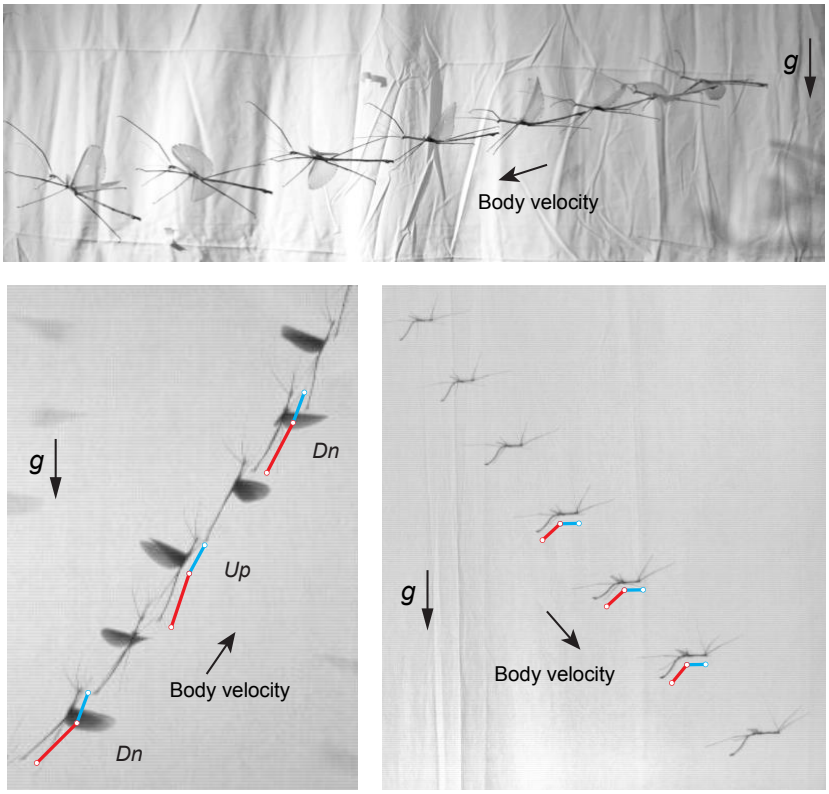

Figure 2. Body-leg posture in stick insect flight.

Sample sequences from flight trials captured with high-speed camera (250 fps; X-PRI, AOS Technologies AG, Switzerland; HiSpec, FasTec Imaging, USA). The top panel shows an *Acrophylla wueferingi* male (L ~13 cm; p_w ~4.3 Nm^{-2}) flying with all legs outspread. The bottom left shows a *Diardia reductipennis* male (L ~12 cm; p_w ~3.8 Nm^{-2}) in ascending flight. Note the oscillation of the abdomen about the median joint. The abdomen flexes downward during upstroke (Up) and reverses during downstroke (Dn), potentially counteracting effects of the oscillatory wing moment. However, these oscillations were not obvious in a gliding, partial-winged species, *Lopaphus iolas* male (bottom right; L ~7.5 cm; p_w ~7.3 Nm^{-2}).

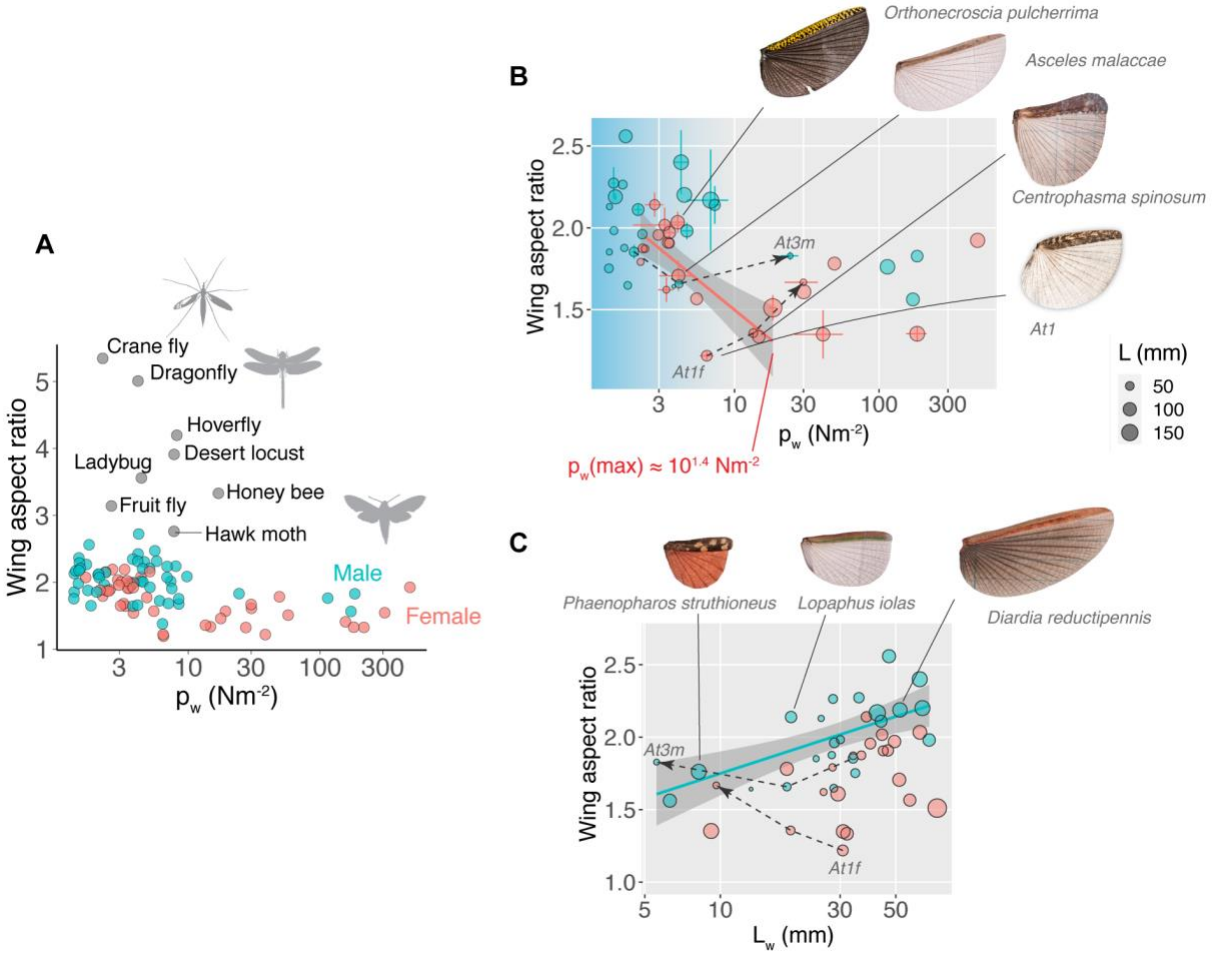

Figure 3. Sex-specific evolution of phasmid wing shape.

(A) A comparison of wing aspect ratio between phasmid taxa sampled in this study (colored dots) and selected winged insects, showing that stick insect wings are of lower aspect ratio compared to other insects of similar wing loading. **(B)** Wing aspect ratio (AR) versus wing loading (p_w) (female, $N = 24$ samples; male, $N = 25$ samples). Colors represent sexes; dot sizes represent body length. Note a clear reduction of AR in wings of females over $p_w > 4$ Nm^{-2}, while wings of male insects show no such reduction. Using a sensitivity analysis (see Methods), we found the strongest correlation in female wings with $p_{w(max)} = 10^{1.4}$ Nm^{-2}, as shown by the trend line here (slope = -0.51±0.14, $P < 0.01$). For males, the correlation between AR and p_w was non-significant and was insensitive to the choice of $p_{w(max)}$. **(C)** The variation of AR with absolute wing length (L_w = LQ), whereby the wings of males exhibited a significant positive correlation (slope = 0.56±0.15; $P < 0.01$) with increasing L_w. In **(B)** and **(C)**, arrows with dashed lines represent variation within *A. tanarata* subspecies along increasing altitude. See **SI Data S2** for phylogenetically justified correlations.

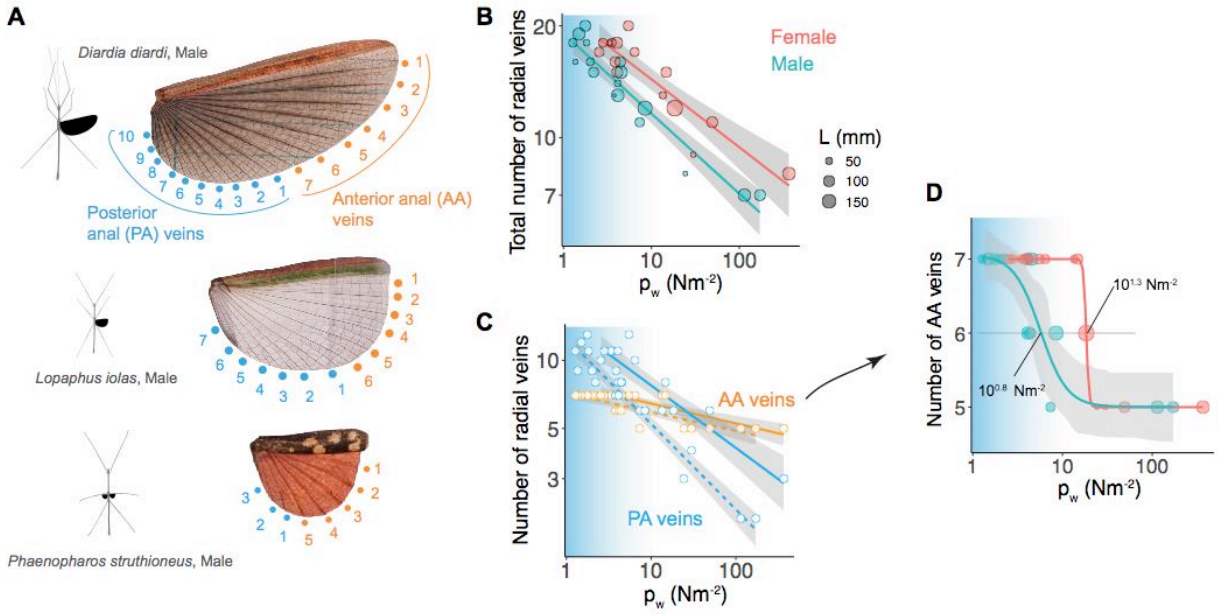

Figure 4. Evolution of stick insect wing venation is coupled with wing loading.

(A) Exemplar wings showing reduction of primary radial veins – anterior anal (AA) and posterior anal (PA) veins. The number of AA veins is conserved, while the number of PA veins varies with relative wing size and wing loading. **(B)** The total number of radial veins (N_V) reduces with increasing wing loading p_w ($N = 34$ female samples; $N = 36$ male samples). Power-law exponent: -5.39±0.80 for females; -5.78±0.66 for males (means±s.e.; $P < 0.0001$ for both sexes). **(C)** Considering two vein groups individually, the number of PA veins varied between 2 – 14 (blue) and is linearly correlated with p_w (female: -0.39±0.04; male: -0.37±0.02), while the number of AA veins (N_{AA}) is more conserved, varying between 5 – 7 (orange). Trend lines are based on linear regression models. **(D)** The transition of N_{AA} from 7 to 5 with increasing p_w, as fitted with sigmoid functions (**SI Data S1**). The model-predicted critical p_w at $N_{AA} = 6$ is $10^{0.75}$ Nm^{-2} and $10^{1.3}$ for males and females, respectively.

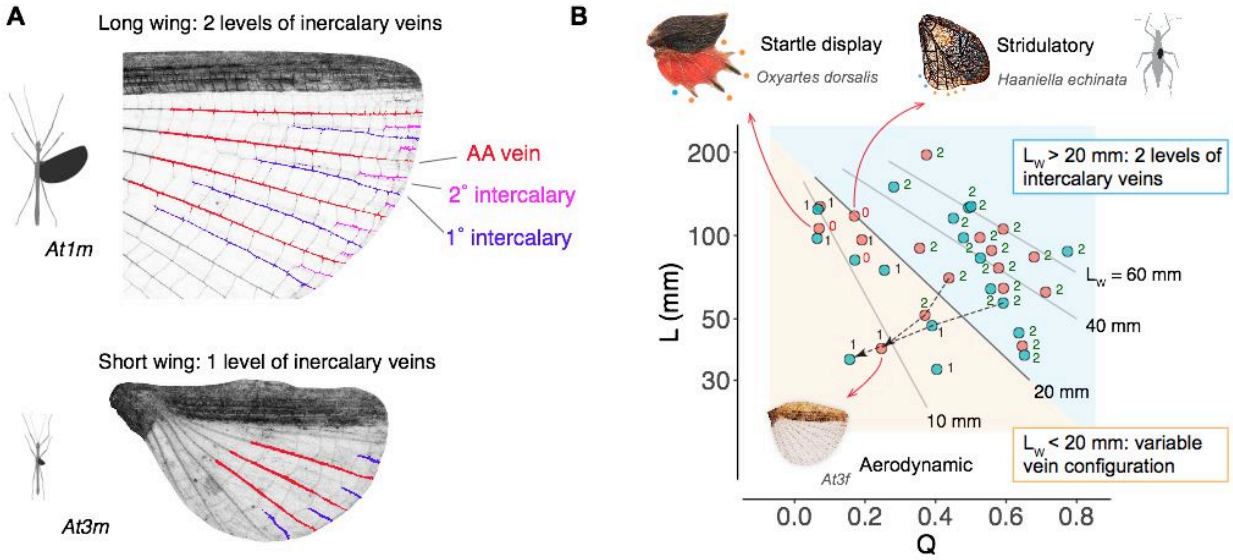

Figure 5. Loss of wing venation hierarchical levels is coupled with wing size reduction.

(A) As gap size between adjacent radial veins increases toward the wing margin, intercalary veins are developed. Long wings possess two levels of intercalary veins, while short wings possess only one, as demonstrated here using At1m and At3m. **(B)** Across all samples, the loss of the 2˚ intercalary vein corresponds with absolute wing length L_w < ~20 mm. Plot shows the levels of intercalary veins as numbers with respect to L and Q, where isolines represent L_w. Relatively more variable venation with derived functions was found in the regime of L_w < 20 mm. Two wings with non-aerodynamic functions and no intercalary veins are annotated on the top, contrasting another wing (from At3f) with 1˚ intercalary veins and potential aerodynamic utility. Values correspond to samples-specific means; dashed lines with arrows show variation in *A. tanarata*.

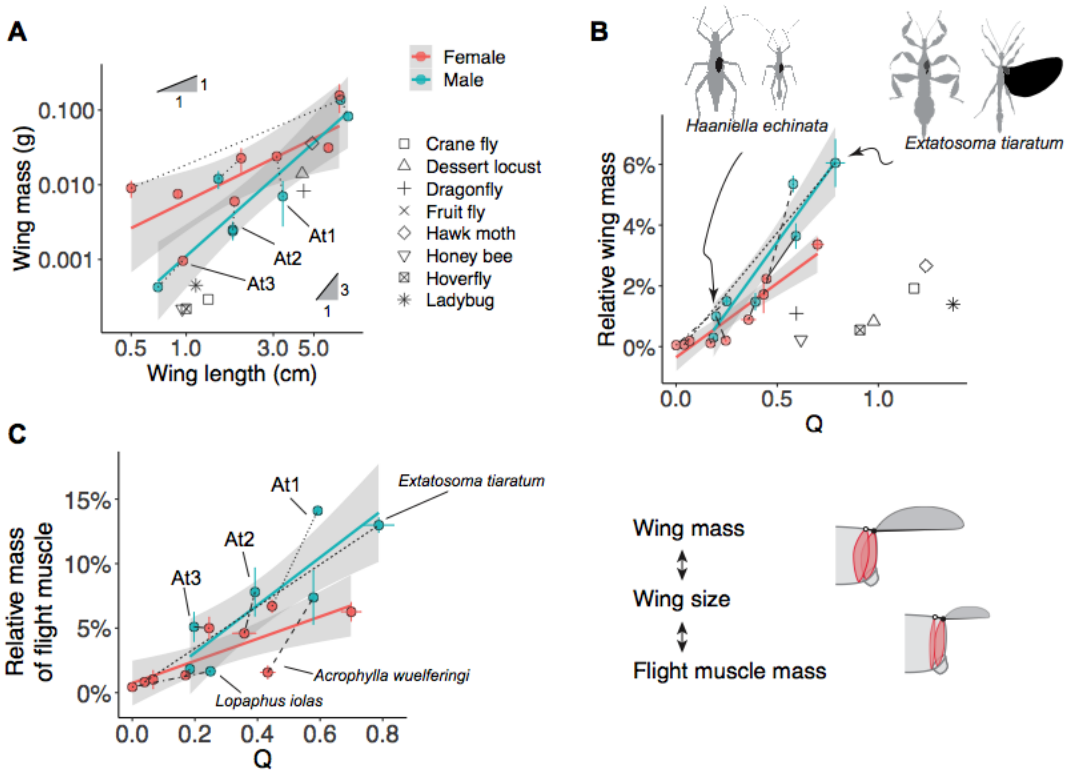

Figure 6. Stick insect wing mass and flight muscle mass.

(A) Sex-specific scaling of the mass of a single hindwing with respect to absolute wing length (L_w) ($N = 9$ female samples; $N = 7$ male samples). Point shape and trend lines represent different sexes; colors represent different species. Females possess heavier wings than males with the same wing size. The power-law exponents (female: 1.2±0.4; male: 2.2±0.4; mean±s.e.) are intermediate to two models: (i) exponent = 3, if dimensions of wings increase isometrically in all three dimensions; (ii) exponent = 1, if wing thickness were conserved and mass is proportional to wing length. **(B)** The power-law scaling of relative wing mass with respect to relative wing size Q, showing that females possess relatively lighter wings than males (Power-law exponents: female, 0.048±0.007; male, 0.092±0.014; mean±s.e.). Compared to other winged insects, stick insects possess relatively shorter but also heavier wings. **(C)** The power-law scaling of flight muscle mass with respect to relative wing size Q, showing that males have greater volume of flight muscle than females (exponent: female, 0.086±0.025; male, 0.185±0.046; mean±s.e.). Values represent sample-specific means±S.D. Trend lines are based on linear regression models; males and females of the same species are connected by dashed or dotted lines.

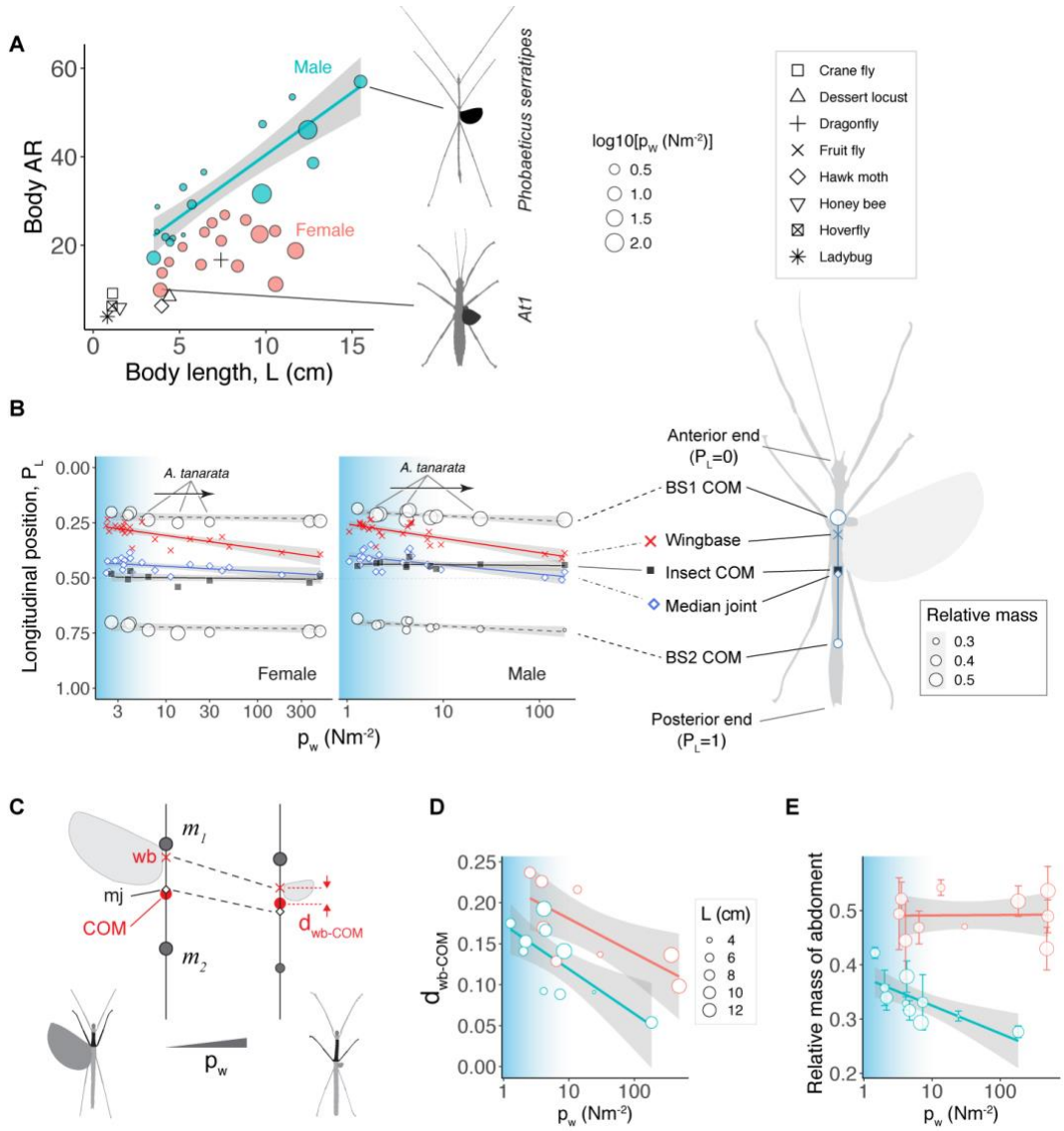

Figure 7. Stick insect bodies vary in slenderness, but flight-related parameters are conserved.

(A) Body aspect ratio (AR; i.e., the ratio of length to mean diameter) versus body length (L) in stick insects and other winged insects. A significant correlation between body AR and L was found in males (slopes = 2.82±0.38; $P < 0.0001$), but not in females ($P > 0.05$). **(B)** Normalized longitudinal positions of flight-related morphological landmarks plotted against wing loading (p_w) for samples (see legend to the right). The positions of the wingbase (red; slope 0.06 – 0.1) and median joint (blue; slope 0.04 – 0.05) shift posteriorly with increasing p_w, while the position of whole-insect COM is relatively unchanged. The size of open dots represents relative mass ($N = 10$ for both male and female samples); trend lines are based on linear regression models ($N = 23$ female samples; $N = 26$ male samples; see **SI Data S1** for details). Black arrows represent three *A. tanarata* subspecies along increasing altitude. **(C)** Schematic demonstration of shifts in wingbase (wb) and median joint (mj) with respect to wing reduction, which is coupled with elongation of the mesothoracic segment (orange), as demonstrated with two exemplar profiles. **(D)** The distance between the wingbase and whole-insect COM ($d_{wb\text{-}COM}$) decreases with increasing p_w in both sexes (slope: females, 0.04±0.02, $P < 0.05$; males, -0.05±0.02, $P < 0.05$). In other winged insects, this parameter is taxon-specific, ranging between 0.12 and 0.26 (Ellington, 1984). **(E)** The relative mass of abdomen decreases with increasing p_w in males, but not in females (males: slope = -0.05±0.02, $P < 0.05$; females: $P = 0.96$).

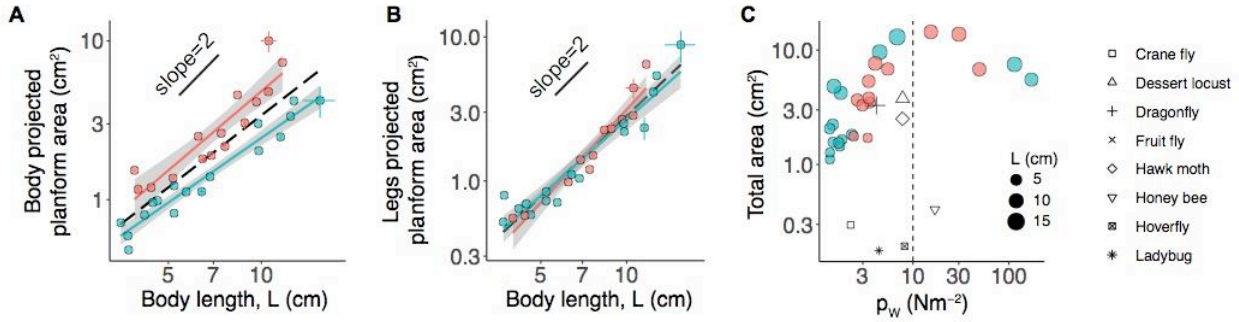

Figure 8. Scaling of projected planform areas for phasmid bodies and legs.

(A) Projected planform area of body sections scales with body size with a sex-averaged power-law exponent 1.54 ± 0.15 (mean±s.e.) (N = 18 female samples; N = 20 male samples). An exponent < 2 suggests disproportionate increase in slenderness as stick insects become longer. The greater slope intercept in females corresponds to wider body segments. **(B)** Projected planform area of all legs exhibits a near-isometry with body length, with a sex-averaged power-law exponent of 1.74±0.13 (mean±s.e.). See **SI Data S1** and **Data S2** for details. **(C)** The total area of the body-leg system during flight versus wing loading p_w, showing that the stick insects have greater aerodynamic surface are compared to winged insects with similar p_w. Dot size represents body length. For other insects, the total projected planform area was estimated based on published data and leg postures in flight (see **SI Data S4**).

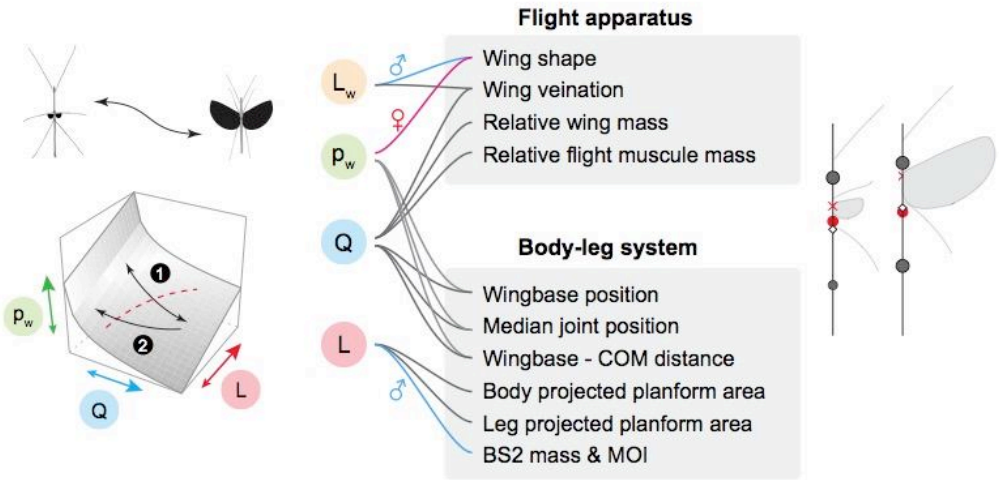

Figure 9. Summary of the evolution of flight-related morphology in stick insects.

(Left) Two types of evolutionary trajectories on the p_w landscape in phasmids: (1) the general inverse correlation between L and Q, and (2) coupled reductions in L and Q exhibited by *A. tanarata* (see **SI Section A** for more details). Gain and loss of flight (most generally represented by p_w) mainly follow the direction of wing size evolution (Q), but are influenced by body size evolution and other sex-specific traits within a variety of ecological contexts. **(Right)** Summary of correlations between morphological and flight-relevant parameters for four principal variables (wing loading, p_w; relative wing size, Q; body size, L; absolute wing size L_w). Colored lines represent sex-specific correlations. See **SI Table S1** for more details.

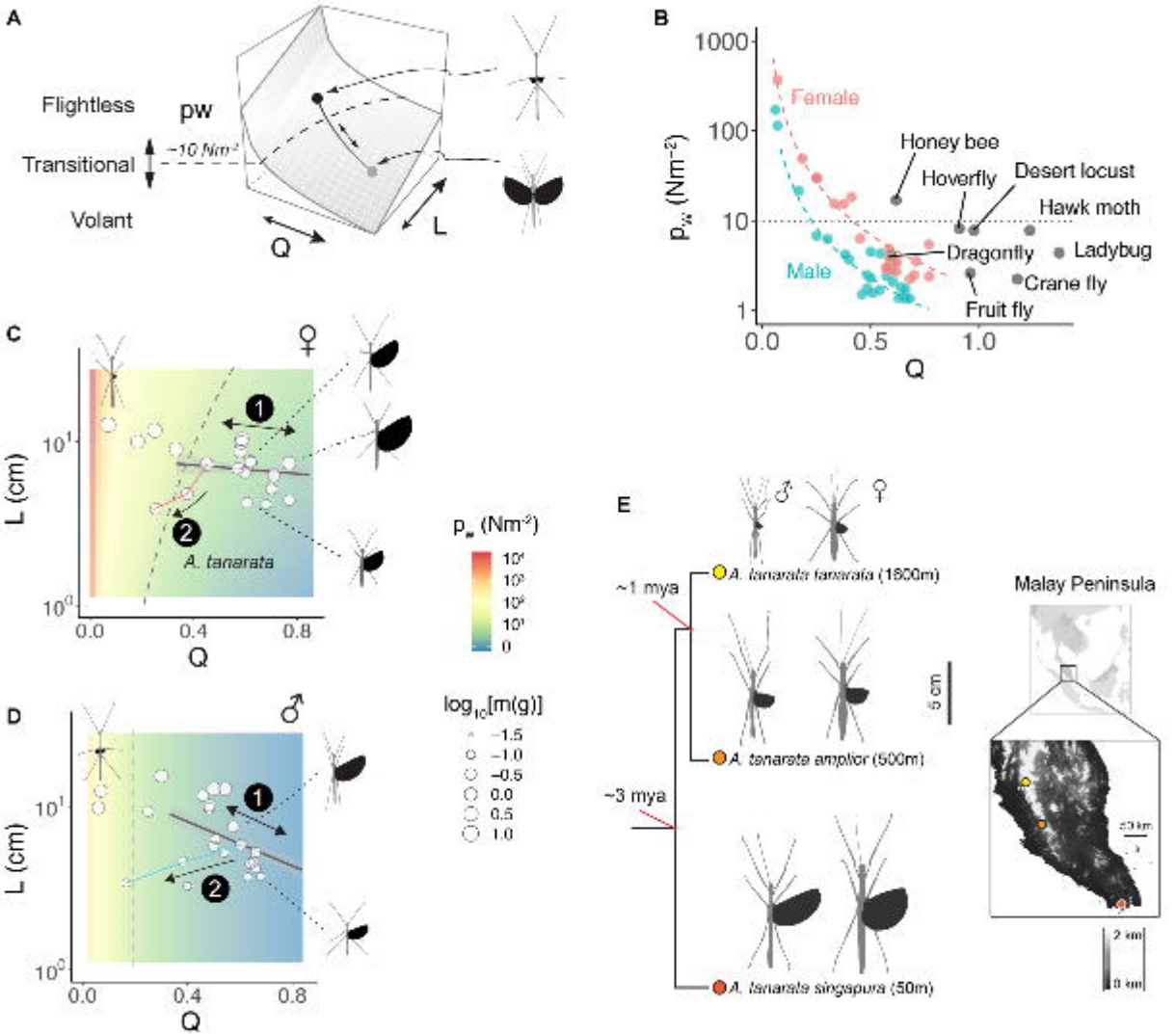
A
Flightless
pw
Transitional
~10 Nm⁻²
Volant
Q
L
B
Female
Male
Honey bee
Hoverfly
Desert locust
Hawk moth
Dragonfly
Ladybug
Crane fly
Fruit fly
p_w (Nm⁻²)
Q
C
♀
L (cm)
A. tanarata
Q
p_w (Nm⁻²)
log10[m(g)]
D
♂
L (cm)
Q
E
♂
♀
A. tanarata tanarata (1800m)
~1 mya
A. tanarata amplior (500m)
5 cm
~3 mya
A. tanarata singapura (50m)
Malay Peninsula
50 km
2 km
0 km

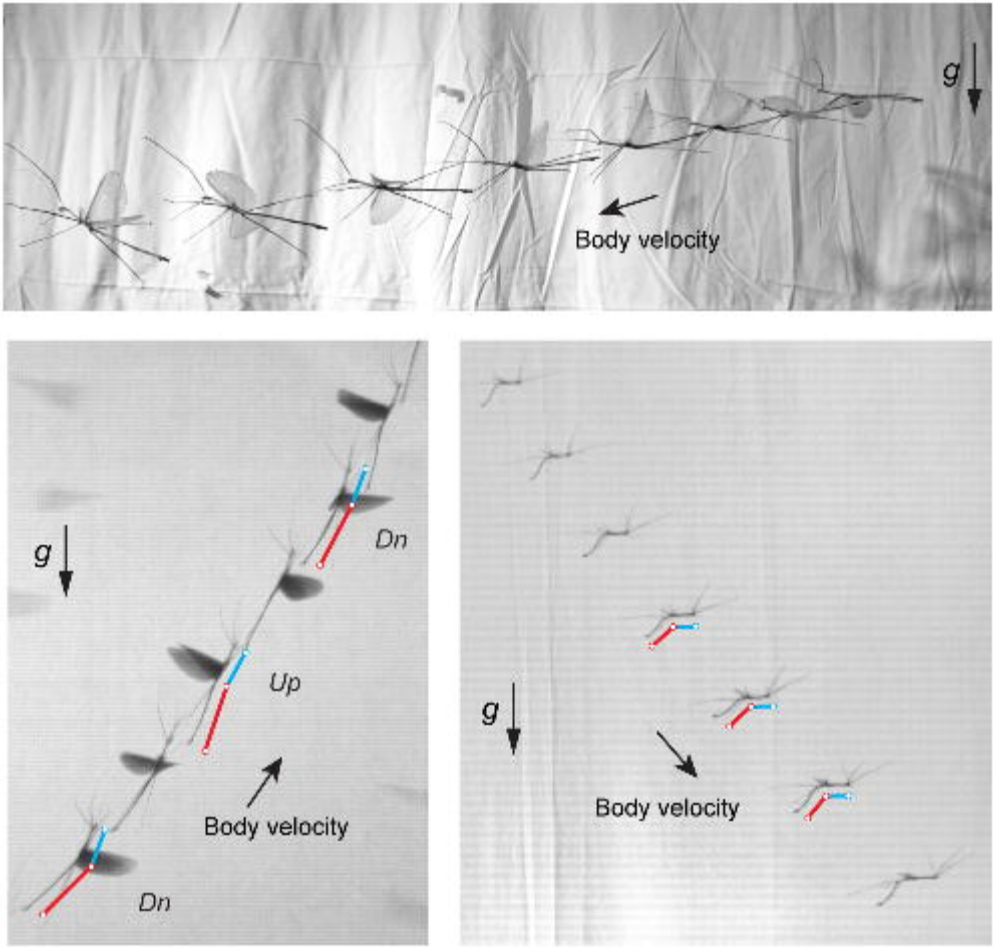
g
Body velocity
g
Dn
Up
Body velocity
Dn
g
Body velocity

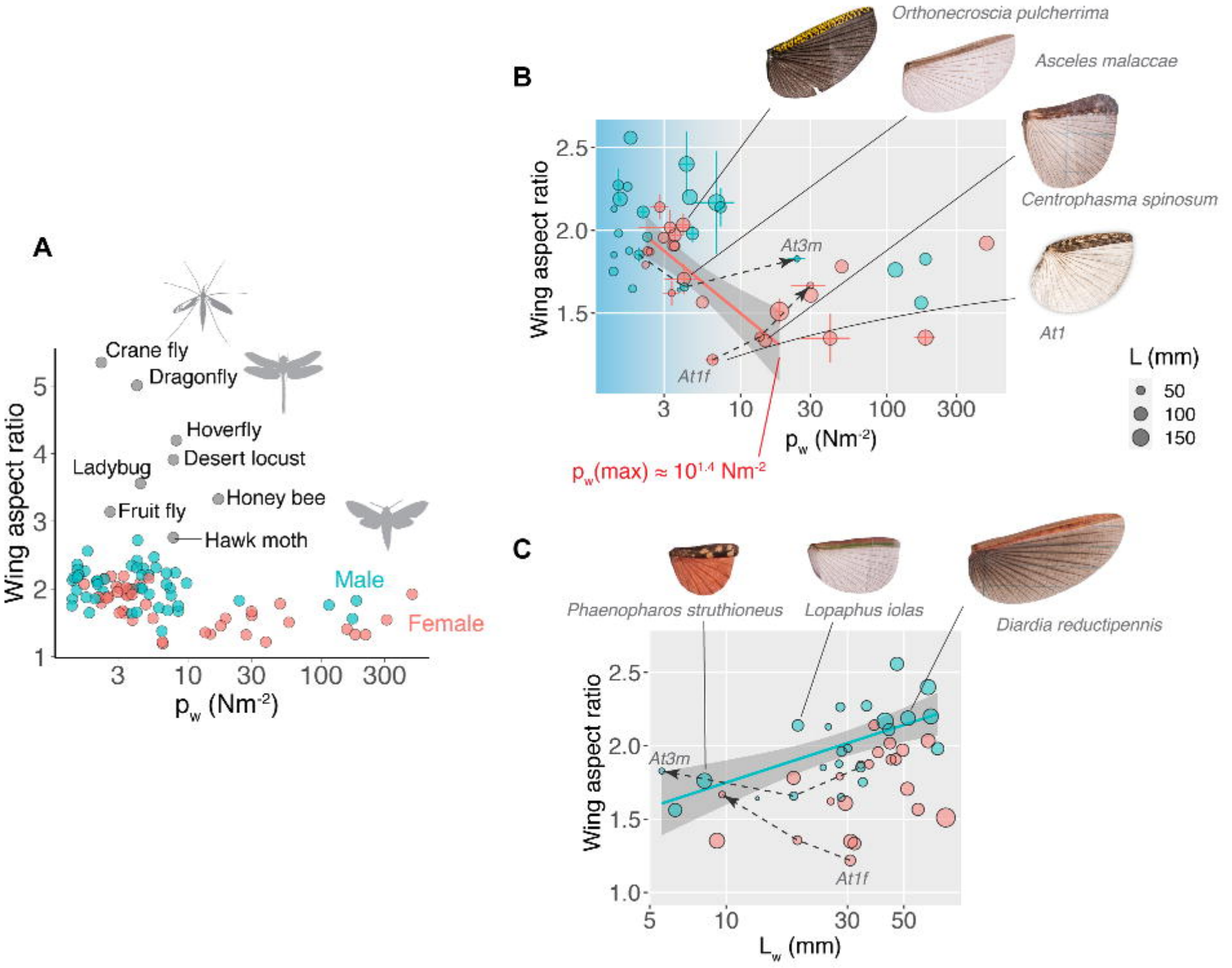
A
Crane fly
Dragonfly
Hoverfly
Desert locust
Ladybug
Honey bee
Fruit fly
Hawk moth
Male
Female
Wing aspect ratio
p_w (Nm^{-2})
B
Orthonecroscia pulcherrima
Asceles malaccae
Centrophasma spinosum
At1
At3m
At1f
Wing aspect ratio
p_w (Nm^{-2})
p_w(max) ≈ $10^{1.4}$ Nm^{-2}
L (mm)
50
100
150
C
Phaenopharos struthioneus
Lopaphus iolas
Diardia reductipennis
At3m
At1f
Wing aspect ratio
L_w (mm)

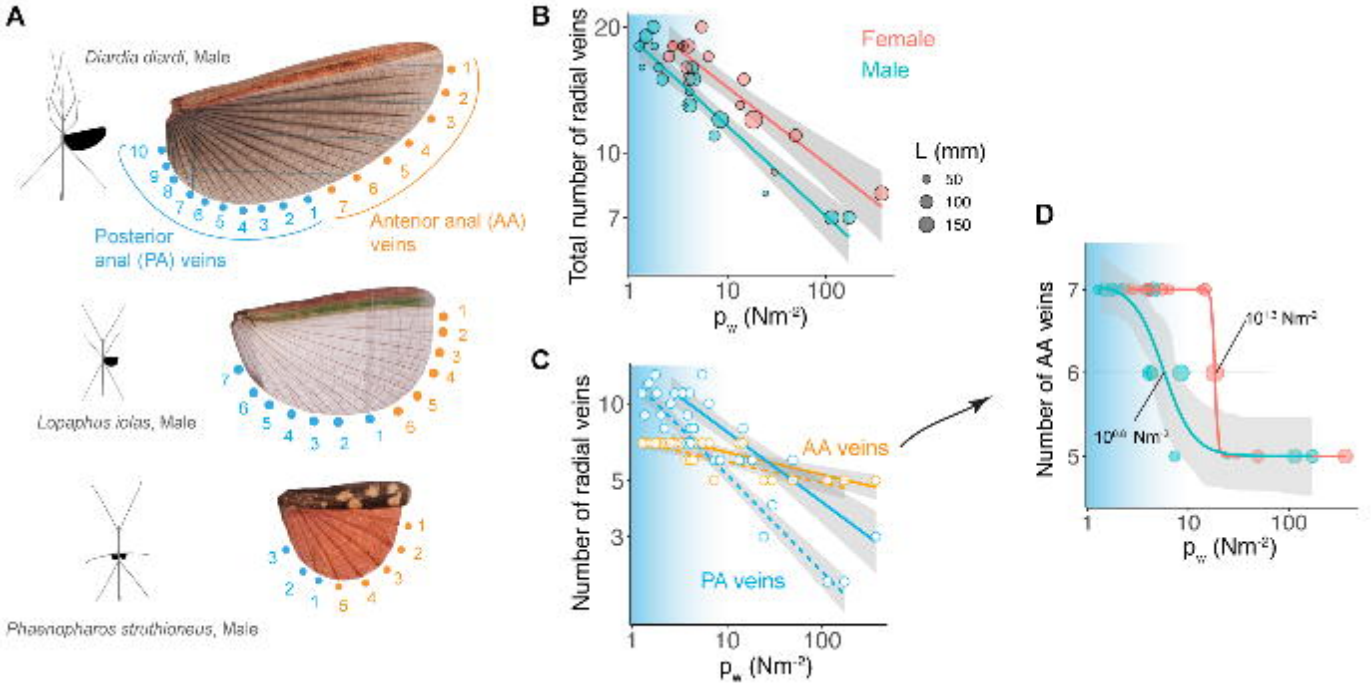

A
Diardia diardi, Male
Posterior anal (PA) veins
Anterior anal (AA) veins
Lopaphus iolas, Male
Phaenopharos struthioneus, Male
B
Total number of radial veins
Female
Male
L (mm)
50
100
150
p_w (Nm^{-2})
C
Number of radial veins
AA veins
PA veins
p_w (Nm^{-2})
D
Number of AA veins
10^{12} Nm^{-2}
$10^{0.6}$ Nm^{-2}
p_w (Nm^{-2})

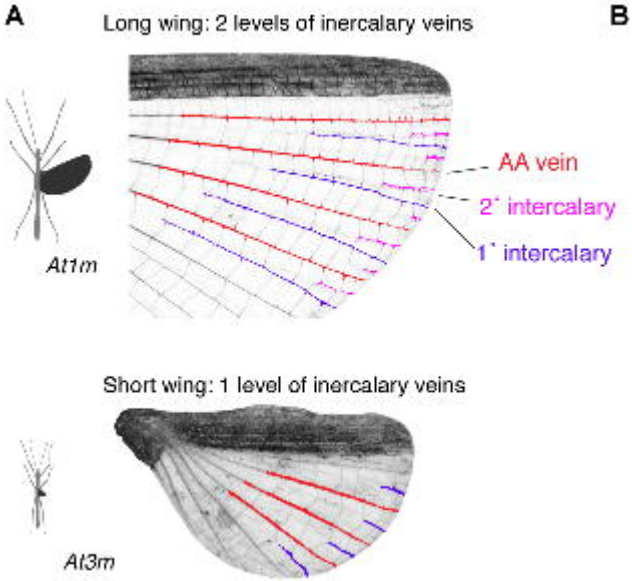
A
Long wing: 2 levels of inercalary veins
At1m
AA vein
2˚ intercalary
1˚ intercalary
Short wing: 1 level of inercalary veins
At3m

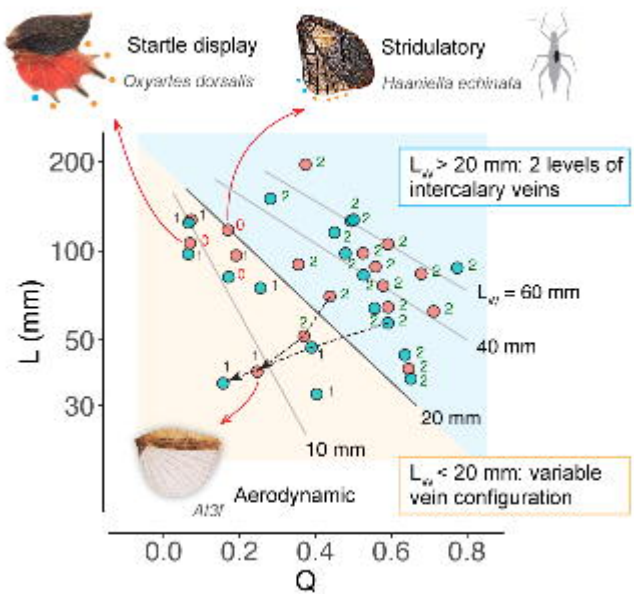
B
Startle display
Oxyartes dorsalis
Stridulatory
Haaniella echinata
L (mm)
200
100
50
30
Q
0.0
0.2
0.4
0.6
0.8
L_w > 20 mm: 2 levels of intercalary veins
L_w = 60 mm
40 mm
20 mm
10 mm
L_w < 20 mm: variable vein configuration
At3f
Aerodynamic

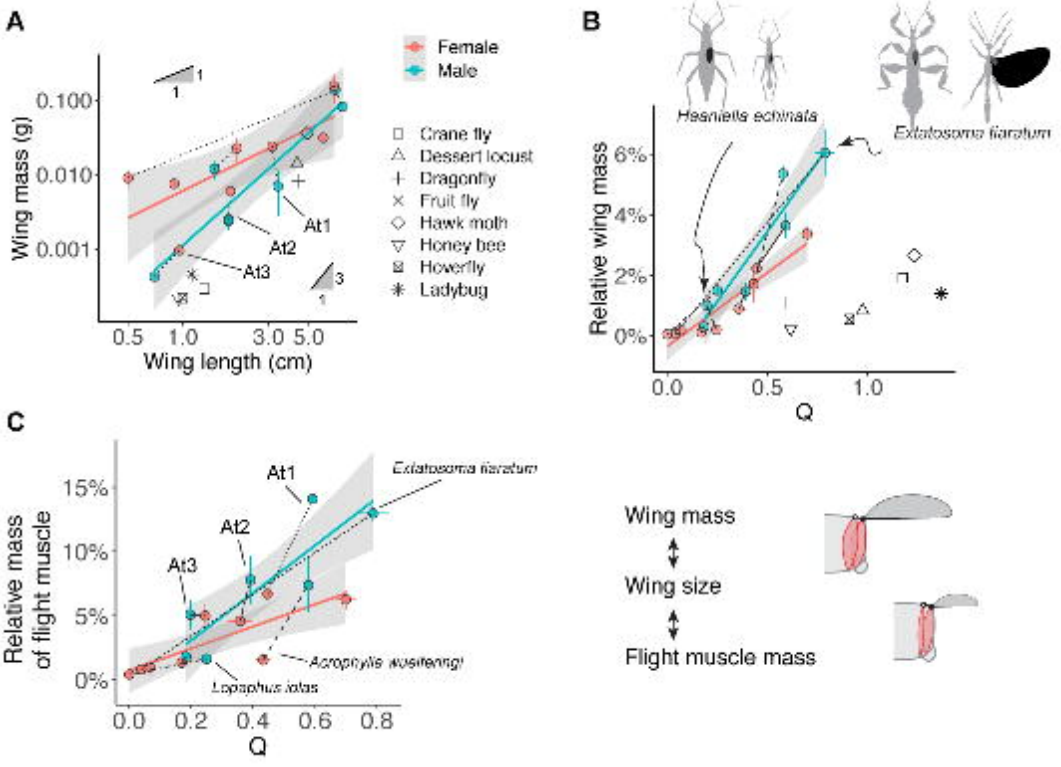
A
Female
Male
Crane fly
Dessert locust
Dragonfly
Fruit fly
Hawk moth
Honey bee
Hoverfly
Ladybug
Wing mass (g)
0.100
0.010
0.001
1
1
3
1
At1
At2
At3
0.5
1.0
3.0
5.0
Wing length (cm)
B
Hesniella echinata
Extatosoma tiaratum
Relative wing mass
6%
4%
2%
0%
0.0
0.5
1.0
Q
C
Relative mass of flight muscle
15%
10%
5%
0%
At1
At2
At3
Extatosoma tiaratum
Acropylis wositenngi
Lopaphus iolas
0.0
0.2
0.4
0.6
0.8
Q
Wing mass
Wing size
Flight muscle mass

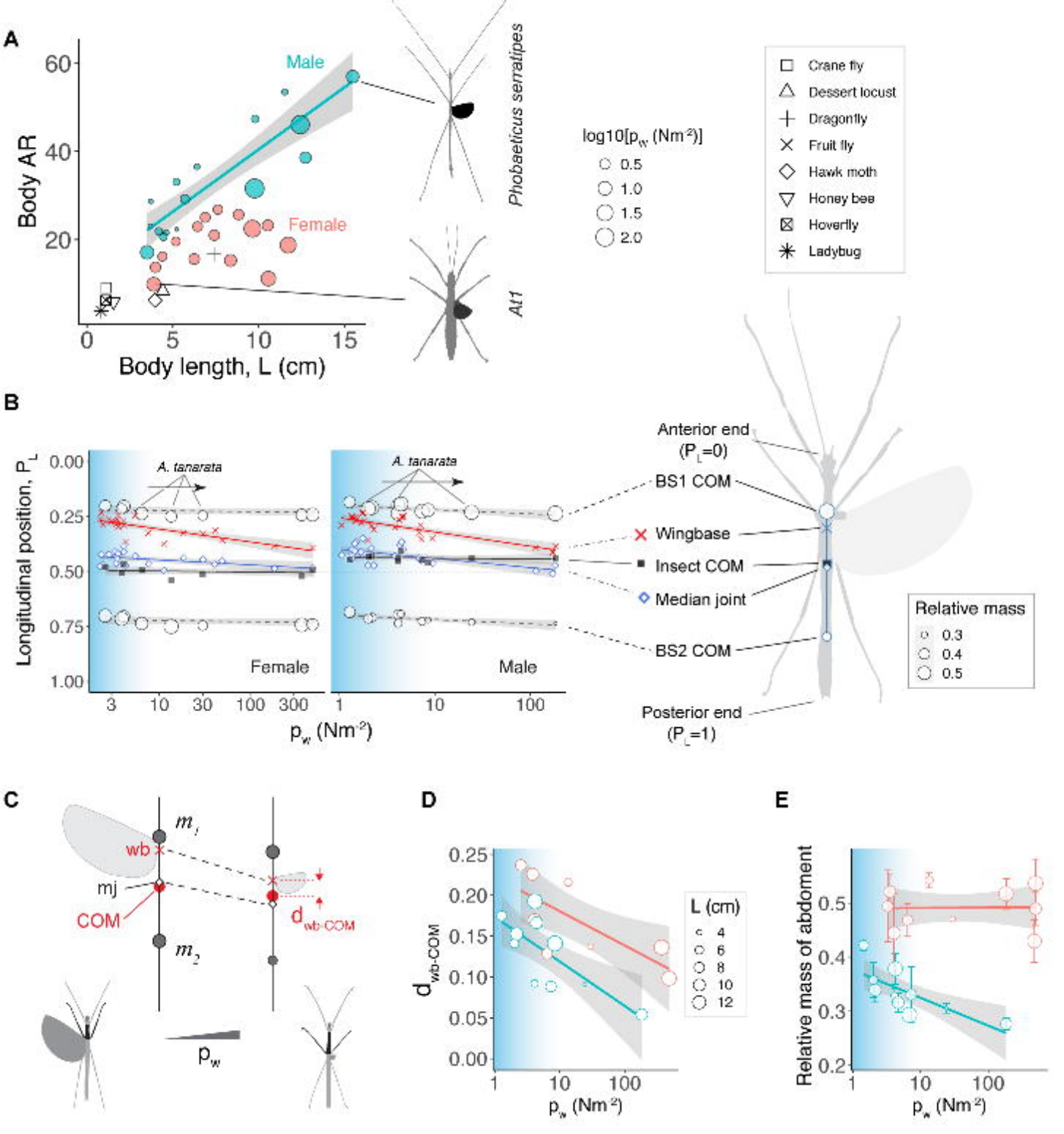
A
Male
Female
Body AR
Body length, L (cm)
Phobaeticus serratipes
At1
log10[p_w (Nm^-2)]
0.5
1.0
1.5
2.0
Crane fly
Dessert locust
Dragonfly
Fruit fly
Hawk moth
Honey bee
Hoverfly
Ladybug
B
Longitudinal position, P_L
A. tanarata
Female
Male
p_w (Nm^-2)
Anterior end (P_L=0)
BS1 COM
Wingbase
Insect COM
Median joint
BS2 COM
Posterior end (P_L=1)
Relative mass
0.3
0.4
0.5
C
m_1
wb
mj
COM
m_2
d_wb-COM
p_w
D
d_wb-COM
L (cm)
4
6
8
10
12
p_w (Nm^-2)
E
Relative mass of abdomen
p_w (Nm^-2)

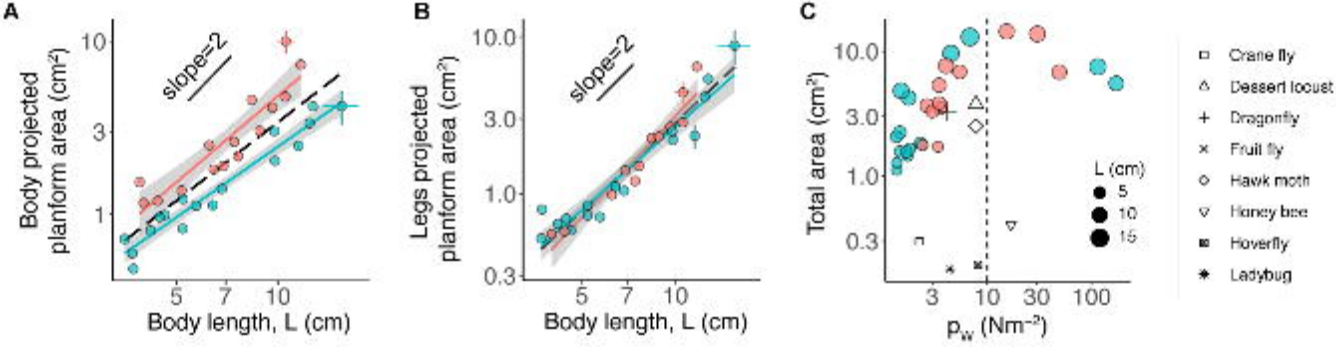
A
Body projected planform area (cm²)
slope=2
10
3
1
5
7
10
Body length, L (cm)
B
Legs projected planform area (cm²)
slope=2
10.0
3.0
1.0
0.3
5
7
10
Body length, L (cm)
C
Total area (cm²)
10.0
3.0
1.0
0.3
3
10
30
100
p_w (Nm⁻²)
L (cm)
5
10
15
Crane fly
Desert locust
Dragonfly
Fruit fly
Hawk moth
Honey bee
Hoverfly
Ladybug

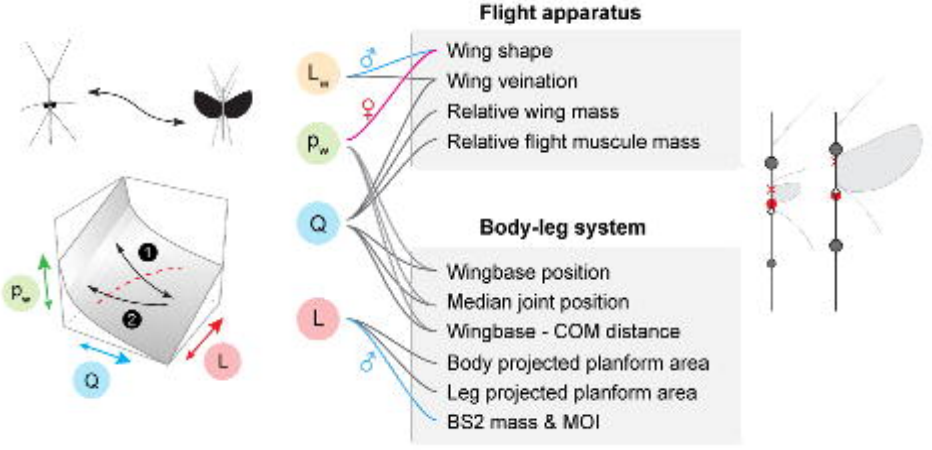
Flight apparatus
Wing shape
Wing veination
Relative wing mass
Relative flight muscule mass
Body-leg system
Wingbase position
Median joint position
Wingbase - COM distance
Body projected planform area
Leg projected planform area
BS2 mass & MOI
L_w
p_w
Q
L
♂
♀
1
2